Astronomy & Astrophysics manuscript no. ms
September 11, 2014
©ESO 2014

arXiv:1409.2869v1 [astro-ph.EP] 9 Sep 2014

SPOTS: The Search for Planets Orbiting Two Stars

I. Survey description and first observations⋆

C. Thalmann[1], S. Desidera[2], M. Bonavita[2], M. Janson[3], T. Usuda[4,5], T. Henning[6], R. Köhler[6], J. Carson[7,6], A. Boccaletti[8], C. Bergfors[9], W. Brandner[6], M. Feldt[6], M. Goto[10], H. Klahr[6], F. Marzari[11], and C. Mordasini[6]

[1] Institute for Astronomy, ETH Zurich, Wolfgang-Pauli-Strasse 27, 8093 Zurich, Switzerland
e-mail: thalmann@phys.ethz.ch
[2] INAF – Osservatorio Astronomico di Padova, Vicolo dell'Osservatorio 5, I-35122, Padova, Italy
[3] Astrophysics Research Center, Queen's University Belfast, Belfast, Northern Ireland, UK
[4] National Astronomical Observatory of Japan, 2-21-1 Osawa, Mitaka, 181-8588 Tokyo, Japan
[5] Department of Astronomical Sciences, Graduate University for Advanced Studies (Sokendai), Mitaka, 181-8858 Tokyo, Japan
[6] Max Planck Institute for Astronomy, Königstuhl 17, 69117 Heidelberg, Germany
[7] Department of Physics & Astronomy, College of Charleston, 58 Coming Street, Charleston, SC 29424, USA
[8] Observatoire de Meudon, LESIA, bat 17, 5 pl. J. Janssen, 92195 Meudon, France
[9] Department of Physics & Astronomy, University College London, Gower Street, London WC1E 6BT, UK
[10] Universitätssternwerte München, Scheinerstr. 1, D-81679 Munich, Germany
[11] Dipartimento di Fisica, University of Padova, Via Marzolo 8, 35131 Padova, Italy

Draft version

ABSTRACT

Direct imaging surveys for exoplanets commonly exclude binary stars from their target lists, leaving a large part of the overall planet demography unexplored. To address this gap in our understanding of planet formation and evolution, we have launched the first direct imaging survey dedicated to circumbinary planets: SPOTS, the Search for Planets Orbiting Two Stars. In this paper, we discuss the theoretical context, scientific merit, and technical feasibility of such observations, describe the target sample and observational strategy of our survey, and report on the first results from our pilot survey of 26 targets with the VLT NaCo facility. While we have not found any confirmed substellar companions to date, a number of promising candidate companions remain to be tested for common proper motion in upcoming follow-up observations. We also report on the astrometry of the three resolved binaries in our target sample. This pilot survey constitutes a successful proof of concept for our survey strategy and paves the way for a second stage of exploratory observations with VLT SPHERE.

Key words. planets and satellites: formation – planets and satellites: detection – binaries: close – techniques: high angular resolution

1. Introduction

While binary star systems have traditionally been assumed to be hostile environments for the formation and survival of planets, a growing body of theoretical and observational evidence demonstrates that this is not the case. Most exoplanet surveys based on the Doppler spectroscopy or direct imaging techniques to date have made active efforts to exclude at least some parameter ranges of known binaries from their target lists (e.g., Jones et al. 2002; Wright et al. 2004; Marcy et al. 2005). In particular, binary target stars present technical obstacles to Doppler spectroscopy, which is responsible for most of the confirmed exoplanet discoveries prior to 2014. It may then come as a surprise that, in spite of these selection biases, 78 of the 729 exoplanets listed in the Exoplanets.org database (Wright et al. 2011) by November 2013 reside in a multiple system, indicating a large and mostly unexplored population of such planets.

Various theoretical and observational studies have been conducted on the impact of binarity on the properties of planets (see e.g. the book "Planets in Binaries", Haghighipour 2010). Since most of these studies are based on Doppler spectroscopy ('radial velocity') observations, they focus on planets on short-period circumstellar (s-type) orbits around components of wide binary systems. The presence of a distant companion star is expected to influence the planet formation process in such systems through truncation and dynamical heating of the protoplanetary disk (e.g., Artymowicz & Lubow 1994). The main result of these studies is that binarity may change the shape of the planet demography, but only slightly impacts the overall frequency of planets (Bonavita & Desidera 2007; Bergfors et al. 2013). However, there are hints that binary companions with separations $\lesssim$ 100 AU, for which these dynamical effects are enhanced, may reduce the number of giant planets formed (see e.g. Bonavita & Desidera 2007; Eggenberger et al. 2007; Wang et al. 2014) and leave a characteristic imprint on their properties (Desidera & Barbieri 2007). However, the available data on such systems is currently still too limited to confirm these hypotheses. In any case, the discovery of circumstellar planets in binary systems with separations as small as ~20 AU (Hatzes et al. 2003; Chauvin et al. 2011), whose existence presents a considerable challenge to current planet formation theories (Thebault 2011),

⋆ Based on data collected at the European Southern Observatory, Chile (ESO Programmes 088.C-0291 and 090.C-0416) and at the Subaru Telescope, which is operated by the National Astronomical Observatory of Japan.

proves that planet formation can succeed even in dynamically excited environments.

In general, planetary orbits in a binary system are stable on long time scales if the overall system architecture is strongly hierarchical (Holman & Wiegert 1999). In the case of circumstellar (s-type) planet orbits, this means that the planet's semimajor axis a must be smaller than a critical upper limit a_c, which in turn is a fraction of the binary's separation a_b depending on the binary's mass ratio and eccentricity. In sufficiently close binary systems ($a_b \lesssim 5$–10 AU), a second regime of stable planet orbits become viable: *circumbinary* (p-type) orbits, which enclose the orbits of both stellar components of the binary host system. In this regime, the stability criterion takes the form of a lower limit on the planet's semimajor axis, $a > a_c$, with a_c/a_b ranging from 2 to 4.

Since the detectability of a planet with transit photometry and Doppler spectroscopy is highly biased towards small semimajor axes, circumbinary planets are generally more challenging to detect with these techniques than circumstellar planets. Despite this disadvantage, seven transiting circumbinary planets have been discovered by the Kepler mission (e.g., Doyle et al. 2011; Orosz et al. 2012), including a multi-planet system and a planet in the habitable zone, hinting at a rich and varied, yet largely undiscovered population of circumbinary planets (Welsh et al. 2013; Armstrong et al. 2014). Several other circumbinary planet candidates were discovered on the basis of eclipse timing variations in post-common-envelope binary systems (e.g., Lee et al. 2009; Beuermann et al. 2010). Some of these claims have been disputed (e.g., Horner et al. 2013), but for at least one target, NN Ser, the evidence for circumbinary planets appears robust (Marsh et al. 2014). It has been suggested that at least some of these planets might have formed as second-generation planets from ejected stellar material after the common-envelope phase (Perets 2010). Efforts are also made to search for circumbinary planets with Doppler spectroscopy (Konacki et al. 2009).

All of these indirect planet detection techniques are heavily biased towards short-period planets, and do not provide meaningful constraints beyond orbital radii of 5–10 AU. On the other hand, direct imaging powered by adaptive optics and differential imaging techniques has proven to be a powerful technique to probe the outer reaches of stellar systems for giant planets (e.g. Neuhäuser et al. 2003; Lafrenière et al. 2007a; Vigan et al. 2012; Rameau et al. 2013a; Biller et al. 2013; Janson et al. 2013), leading to a number of discoveries of planets (e.g. Lagrange et al. 2010; Marois et al. 2010; Carson et al. 2013; Kuzuhara et al. 2013; Rameau et al. 2013b) and brown-dwarf companions (e.g. Thalmann et al. 2009; Biller et al. 2010). However, the published imaging surveys have largely avoided close binary targets, leaving a vast unexplored territory in the parameter space of circumbinary planets. While Crepp et al. (2010) target narrow binaries in search of circumbinary tertiary bodies, their sensitivity is limited to stellar companions. Delorme et al. (2013) reported the imaging discovery of a 12–14 M_{Jup} substellar companion orbiting a pair of M-dwarf stars, though the comparatively high mass ratio implies a stellar rather than planetary origin. To date, no *bona fide* circumbinary planet has been imaged.

The SPOTS project (Search for Planets Orbiting Two Stars; Thalmann et al. 2013) aims to fill in this gap by conducting the first direct imaging survey dedicated to circumbinary planets. In a first stage, 26 nearby young spectroscopic binary targets have been observed over the past 2 years with VLT NaCo, and 41 more targets are foreseen for a second stage using VLT SPHERE in the coming 2–3 years. In this work, we present the scientific justification, observing strategy, and preliminary results for the first stage of the SPOTS survey. Due to the unavailability of NaCo in ESO periods P92 and P93, the follow-up efforts for this stage are still ongoing; thus, final observational results and statistical analysis will be presented in a future publication. Furthermore, we complement our survey with a comprehensive census of the body of archival high-contrast imaging data of spectroscopic binary targets (Bonavita et al. 2014, herafter Paper II), including a detailed statistical analysis based on the `MESS` code (Bonavita et al. 2011).

In Section 2, we discuss the scientific merit of direct imaging of circumbinary planets in more detail. Section 3 describes the survey design and lists the targets covered by the first stage of SPOTS. We report on our high-contrast observations and their preliminary results in Section 4, and summarize our conclusions in Section 5.

2. The science case for direct imaging of circumbinary planets

As outlined in Thalmann et al. (2013), the scientific motivation of the SPOTS project to search for circumbinary planets by direct imaging can be summarized in the following four points.

2.1. Unexplored territory

Since stellar binarity is wide-spread, with approximately half of all Sun-like stars having a stellar companion (Raghavan et al. 2010), circumbinary planets may constitute a significant fraction of the overall planet population. In the spirit of fundamental research, it is therefore inherently interesting to explore this largely unknown parameter space.

The existence of circumbinary planets is favored by both observational and theoretical arguments. For instance, the existence of circumbinary disks (Mathieu 1992; Dutrey et al. 1994) and the growth and crystalization of dust in such disks (Pascucci et al. 2008; Duchêne et al. 2004) are well attested, and thus provide the necessary ingredients for planet formation. While secular excitation of planetesimal orbits driven by the binary has been proposed as an obstacle to core accretion, favoring erosion over accretion (Meschiari 2012), Rafikov (2013) proposes that the asymmetric gas disk in such a system dampens the excitation and promotes accretion. Marzari et al. (2013) instead finds that the overall effect of the eccentric disk on the planetesimal population is destructive, whereas Martin et al. (2013) find that a 'dead zone' within a layered circumbinary disk may promote accretion, and even locally render planet formation more efficient than at similar separations around single stars. In any case, the discovery of seven transiting circumbinary planets with Kepler (Welsh et al. 2013) demonstrates that planet formation does successfully occur in close circumbinary configurations. Furthermore, direct imaging is sensitive to planets in wider orbits, where the perturbing influence of the central binary decreases.

2.2. Good observability with direct imaging

Unlike Doppler spectroscopy and transit photometry, direct imaging does not suffer technical difficulties from spectroscopic binary targets. As long as the binary is not resolved, it behaves like a single star for the purposes of adaptive optics guidance and differential imaging methods. Resolved binaries may achieve comparable performance if the secondary star is significantly fainter than the primary, as observations from our SPOTS pilot survey demonstrate (Section 4). These observational constraints

coincide with the ideal conditions for stable circumbinary planet orbits (close stellar separation and/or high stellar mass ratio; Holman & Wiegert 1999), and are therefore compatible with most astrophysically promising targets.

Furthermore, circumbinary planets may offer a distinct advantage in terms of contrast. The number of massive planets formed in a system is thought to scale with the available mass of the protoplanetary disk, which in turn scales with the mass of the host star (e.g Kennedy & Kenyon 2008). This notion is supported empirically by the fact that the majority of directly imaged planets have been found around early-type host stars (Lagrange et al. 2010; Marois et al. 2010; Carson et al. 2013; Rameau et al. 2013b). If this relation also holds for close binary stars, then a pair of G-type stars should offer the same planet-forming resources as a single A-type. However, the former system is several magnitudes fainter than the latter, and thus offers much more favorable conditions for direct imaging of self-luminous planets.

2.3. More planets on wide orbits?

Close binary systems offer two mechanisms that may increase the number of planets on wide orbits, which are the favored targets of direct imaging.

Scattering. Planets forming or migrating close to the inner edge of the stability region may experience a close encounter with the host system's secondary star, which results in dynamical scattering of the planet (Nelson 2003; Veras & Armitage 2004). While most of these events end with the ejection of the planet from the system, some produce highly eccentric, bound orbits with large semimajor axes. These planets may subsequently be damped into less eccentric wide orbits through interaction with the protoplanetary disk.

Numerical simulations by Pierens & Nelson (2008) suggest that massive giant planets ($\geq 1\,M_{\rm Jup}$), which make favorable objects for direct imaging, are particularly prone to scattering, whereas lower-mass planets may instead remain stranded near the inner edge of the stability region (see also Pierens & Nelson 2013; Kley & Haghighipour 2014). This prediction has received some observational support in a recent study by Armstrong et al. (2014) on Kepler transit photometry data, which indicates that the frequency of small planets (radius smaller than Jupiter's) on short orbits (periods ≤ 300 d) is consistent between tight binary and single host stars, but that Jovian-sized planets appear significantly depleted in the circumbinary case. Considering that the high system mass of binary systems is thought to favor the formation of massive planets (cf. Section 2.2), these findings suggest a selective depletion mechanism for such planets consistent with Pierens & Nelson (2008).

Migration. A second possibility is continuous outward migration as opposed to isolated scattering events (Martin et al. 2007). This requires transfer of angular momentum from the host binary to a planet via viscous disk interaction, rendering the binary orbit tighter and the planet orbit wider. Due to the low mass ratio between the planet and the stars and the nonlinearity of the gravitational potential, a small change in the binary orbit has a large effect on the planet orbit, which may extend out to 20–50 AU.

While the chances of either process occurring in a system may be low, one must keep in mind that giant planets in wide orbits are rare to begin with (Nielsen & Close 2010); thus these mechanisms may still result in a measurable enrichment of the population of such planets.

2.4. Improved constraints on planet formation theories

Circumbinary systems provide an excellent laboratory for testing theories of planet formation and evolution. Theoretical studies have predicted both positive and negative effects of binarity on planet formation, in both the core accretion scenario (e.g., Marzari et al. 2013; Martin et al. 2013) and the gravitational instability scenario (Mayer et al. 2005; Boss 2006). Such effects are expected to leave characteristic imprints on the planet demography around binary systems. Measuring those differences to the planet demography around single stars may then provide insights into the underlying physical processes. Similar studies for circumstellar planets in wide binaries have already found tentative evidence for such differences (e.g., Bonavita & Desidera 2007).

For circumbinary planets, a first indication of such a demographic feature is found in Kepler transit photometry data, where circumbinary planets have so far been found exclusively in host systems with binary orbital periods $P_{\rm bin} \leq 7$ d, although the detection bias from sampling coverage favors target binaries with shorter periods (Welsh et al. 2013; Armstrong et al. 2014). Possible explanations for this feature include reduced detectability of planets orbiting short-period binaries due to a larger spread of orbital misalignment, reduced planet formation efficiency due to higher secular perturbations in such systems, or loss of planets to dynamic scattering in the formation phase of the short-period binary. Sampling the circumbinary planet demography with direct imaging could test whether this effect extends to wide planet orbits, and thus help identify underlying astrophysical causes.

3. Survey design

3.1. Target selection

The selection of targets was based on an extensive compilation of nearby young stars assembled in preparation of the SPHERE guaranteed-time survey. The indication of young age is derived from various indicators such as membership to young moving groups, lithium content, chromospheric and coronal emission, and fast rotation. From this list we selected 67 young spectroscopic and close visual binaries as suitable targets for a direct-imaging search for circumbinary planets. As a selection criterion, we demanded that the background-limited minimum detectable planet mass in a one-hour NaCo observation be $\leq 5 M_{\rm Jup}$. This imposes joint constraints on the distance and age of the target systems, allowing higher ages for more nearby stars. For early-type target stars, which are expected to form higher-mass planets than Sun-like stars, this criterion was relaxed to $\leq 8 M_{\rm Jup}$. The median minimum detectable planet mass was below $1 M_{\rm Jup}$ for the Moving Groups subsample, $2.8 M_{\rm Jup}$ for the Field Stars subsample, and $4.4 M_{\rm Jup}$ for the Early-Type subsample. A total of 26 targets were eventually observed in the NaCo stage of the SPOTS survey.

It should be noted that close tidally-locked binaries are characterized by high levels of chromospheric and coronal emission and fast rotation even at old ages, mimicking the appearence of young stars. Indeed, several old tidally-locked binaries are included in previous direct-imaging surveys (Paper II). To exclude this kind of systems, which are not suited for our science aim, we required that the estimate of young age not be based solely on activity and rotation, but also on other indicators such as lithium content and group membership, unless the availability of the binary orbital elements (e.g., long period) allowed to rule out the tidal-locking scenario. We should mention, however, that lithium

Table 1. Target list for the NaCo-based stage of the SPOTS survey.

Name	RA(2000)	Dec(2000)	Dist (pc)	Age (Myrs)	H (mag)	SpT	$M_{\rm star}$ ($M_\odot$)	$M_{\rm comp}$ ($M_\odot$)	ρ (arcsecs)	P (days)	e	$a_{\rm crit}$ (AU)	Notes
HIP 9892 = HD 13183	02:07 18.10	-53:11:56.00	50.9	30									
HIP 12545	02:41:25.90	+05:59:18.40	42.0	16	7.20	M...	0.76		–	–	–	< 20	
UX For = HIP 12716	02 43 25.57	-37:55 42.53	40.7	600	6.10	G6V+	0.88	0.64		0.95	0.00	0.05	Triple
							0.88+0.64	0.58	0.38	–	–	71.3	Triple
HIP 16853 = HD 22705	03:36:53.40	-49:57:28.90	41.7	30	6.26	G2V	1.0	0.40	–	201.0	0.00	1.77	
V1136 Tau = CHR 14 = HD 284163	04 11 56.22	+23:38:10.76	38.1	625		K0	0.78+0.49	0.52	0.31	40y	0.853	51.1	Triple
TYC 5907-1244-1	04:52:49.50	-19:55 02.00	72.0	30	7.50	K1Ve	0.87		–	–	–	< 10	
AF Lep = HIP 25486	05:27:04.76	-11:54;03.47	27.0	16	2.93	F7V	1.06	0.76[a]	–	–	–	< 10	
HIP 25709 = HD 36329	05:29:24.10	-34:30:56.00	70.9	30		G3V	1.07					< 10	
XZ Pic = HIP 27134	05:45:13.40	-59:55:26.00	49.8	300		K0V(e)	0.95	–	–	–	–	< 1	
Alhena = γ Gem = HIP 31681	06:37:42.71	+16:23:57.41	33.5	300	1.84	A1.5IV+	3.0	1.0	0.273	12.63yr	0.89	40	
TYC 8104 0991 1	06:39:05.70	-45:12:58.00	56.5	100	8.25	K3Ve	0.83	–	–	–	–		
26 Gem = HIP 32104	06:42:24.33	+17:38:43.11	43.6	30	5.07	A2V	2.70	0.51	–	522	0.10	4.76	
EM Cha = RECX7	08:43:07.24	-79:04:52.50	97.0	8	7.75	K7Ve	1.0	0.4	–	2.6	–	0.10	
TYC 8569 3597 1	08:51:56.40	-53:55:57.00	141.0	30		G9V	1.11		–	24.06	–	< 1	
GS Leo = HIP 46637	09:30:35.83	10:36:06.25	42.3	300	6.69	G5	0.89	–	–	–	–	< 1	Wide comp.
TYC 9399 2452 1	09:19 24.00	-77:38:45.00	56.8	800	7.56	K0IVe	0.96	–	–		–	< 1	Wide comp.
HIP 47760 = HD 84323	09:44:14.10	-11:52:21.00	76.3	30		G3V	1.08	–	–	–	–	< 10	
TYC 6604 0118 1	09:59:08.40	-22:39:35.00	61.1	100	7.49	K2Ve	0.83	0.74	–	1.84	0.00	0.08	
HS Lup = HIP 74049	15:07 57.75	-45:34:45.84	45.1	250		G5IV+G5IV	1.03		–	17.83	0.20		
HIP 76629 = HD 133822	15:38:57.50	-57:42:27.00	38.5	16		K0V	1.12	~0.11	–	~4.5 yr	~0.5	~10.9	Wide comp.
HIP 78416 = HD 143215	16:00 31.32	-36:05 16.62	84.39	16		G1V	1.22		–	–	–	< 10	Wide comp.
BS Ind = HIP 105404	21:20:59.80	-52:28:40.10	45.15	30	6.70	K0V	0.90	0.80	–	1223	0.60	10.23	Triple
IK Peg	21:26:26.66	+19:22:32.30	46.36	100		A8m+DA	1.45	0.99	–	21.72	0.00	0.45	
δ Cap	21:47:02.44	-16:07:38.23	11.87	540	2.01	A5	1.50	0.56	–	1.0	0.01	0.06	
CS Gru = HIP 109901	22:15:35.20	-39:00 51.00	56.10	100	7.12	K0V	0.89	0.45	–	–	–	< 10	
TYC 6386 0896 1	22:44:38.90	-15:56:29.00	57.9	150	7.47	K1Ve	0.88		–	–	–	< 1	

content can also be altered in close binaries, making the age estimate challenging (Pallavicini et al. 1992).

Table 1 summarizes the stellar and binary parameters of the observed target sample. The determination of the stellar parameters follows the methods described in Desidera et al. (2014). We listed the mass of the binary companion and the orbital elements where available. We also derived the critical semimajor axis for dynamical stability (Holman & Wiegert 1999), to have an estimate of the minimum separation at which circumbinary planets can be found in stable orbits. In most cases, the results were significantly smaller than the inner working angle of our imaging observations. Where orbital elements are not available, upper limits based on, e.g., the observed radial velocity variability are listed. The targets are also described individually in Appendix A.

3.2. Observing strategy

For the first stage of the SPOTS survey, we make use of the Very Large Telescope (VLT) NAOS-Conica (NaCo) high-contrast adaptive-optics (AO) imaging facility. We follow the observing technique that was used for the NaCo Large Program (Chauvin et al. 2014; ESO programs 184.C-0567, 089.C-0137, 090.C-0252), a direct imaging survey for planets around single stars, whose observational stage has been completed successfully and whose concluding publications are currently in preparation. Analogous observing strategies are employed by other surveys as well, such as the ongoing SEEDS survey on Subaru HiCIAO (Tamura 2009).

For each survey target, an exploratory H-band (1.6 μm) high-contrast imaging observation is taken on VLT NaCo. If the data reduction reveals faint point sources at significance levels of $\geq 5\,\sigma$ with convincing visual characteristics in the vicinity of the target star, a second epoch of observation must be taken in order to test these companion candidates for common proper motion with the target star. From our experience with the NaCo Large Program, we expect roughly 30% of all targets to have candidates in need of such astrometric follow-up (Chauvin et al. 2014). The time between the exploratory and follow-up observations is chosen such that the star exhibits a measurable amount of proper and parallactic motion (ideally $\geq$ 100 mas) with respect to the sky background. Due to the slow duty cycle involving proposal-writing and service-mode observation, the practical minimum epoch difference is roughly one year, which is a sufficient amount of time for most target stars. Should any candidates be confirmed as co-moving and thus as physical companions to their stars, further follow-up observations will be pursued.

The exploratory and astrometric follow-up observations follow the same pattern. Each observing block is one hour long, and includes target acquisition, two short four-point dithering sequences of unsaturated images taken with the `ND_short` neutral density filter (transmission 0.0123 ± 0.0005 in H-band, Bonnefoy et al. 2013) for photometric calibration purposes bracketing the science observations, and a sky background observation for fixed-pattern noise calibration towards the end of the observing block. We use the H-band filter and the high-resolution camera with a pixel scale of 13.7 mas and a field of view of 1024 pixels = 14″ across. For two particularly bright targets, the field of view was reduced by half in order to allow for faster detector readout times. The NAOS AO system is run in natural guide star mode and must provide close to diffraction-limited resolution in order to qualify an observing run as successful. Pupil-tracking mode is used in order to allow for angular differential imaging (ADI; Marois et al. 2006) data reduction, and cube-mode data storage is employed to reduce overhead. Due to the limited Strehl ratio in H-band as well as unreliable pointing stability, we forego the use of a coronagraph and instead saturate the target star out to $\sim$ 7 pixels in order to achieve high background-limited sensitivity. The integrated exposure time on the science target is on the order of 40% of the duration of the observing block.

All data sets of this kind are reduced by subtracting a fixed-pattern noise, dividing by a flat field image, binning the ensemble of exposures into a manageable number of master frames if necessary, and finally subtracting the stellar point-spread function (PSF) with the ADI technique using the LOCI algorithm (Locally Optimized Combination of Images; Lafrenière et al. 2007b). Since the aim is to detect point sources, the LOCI parameters are set to aggressive values (tyically, a frame selection criterion of $N_\delta = 0.5$ FWHM and an optimization area of $N_A = 300$ PSF footprints). Fake planet signals are injected into the data in order to measure and compensate for the loss of planet flux due to partial self-subtraction, following the procedure in Lafrenière et al. (2007b). We estimate the hypothetical companion masses for the candidates by comparing their absolute H-band magnitude with the `COND` evolutionary models (Allard et al. 2001; Baraffe et al. 2003).

Companion candidates are identified as faint signals with morphologies compatible with the PSF core and statistical significance of at least $5\,\sigma$. The significance is calculated as the S/N ratio, using a radial noise profile calculated as the standard deviation in concentric annuli around the star.

While the NaCo-based first stage of the SPOTS survey is planned to be concluded in 2015, a second stage covering the remaining 40 targets is foreseen to be executed with VLT SPHERE in the coming years.

4. Observations and preliminary results

4.1. Exploratory observations

A total of 14 and 13 targets were observed with VLT NaCo as part of the SPOTS survey under the ESO programs 088.C-0291(A) and 090.C-0416(B), respectively. Details for these observations are presented in Table 2. For each observed target, the epoch of first observation, the integrated time on target, and the presence of candidates or other notable field objects is noted. The last two columns furthermore note whether the exploratory observations revealed candidates in need of follow-up observations, and whether such follow-up has been obtained successfully at the time of writing. Figure 1 illustrates the high quality of the high-contrast data on the examples of the two targets Alhena and EM Cha, and Figure 2 provides plots of the contrast and minimum detectable planet mass curves for those two targets.

4.2. Follow-up observations

In ESO program 090.C-0416(A), four targets from the P88 exploratory observations flagged for follow-up were observed for a second epoch. In the case of IK Peg, the background-limited sensitivity of the follow-up data was insufficient to re-detect the faint candidates of the first epoch, probably due to worse weather conditions during the second epoch. This observation will therefore have to be repeated.

For the P90 target GS Leo, we pursued special follow-up observations via director's discretionary time (DDT) on the Subaru IRCS facility (Kobayashi et al. 2000). This target lies in the Northern hemisphere and thus passes close to zenith when viewed from the Mauna Kea observatory, affording a much higher field rotation rate and thus superior ADI performance

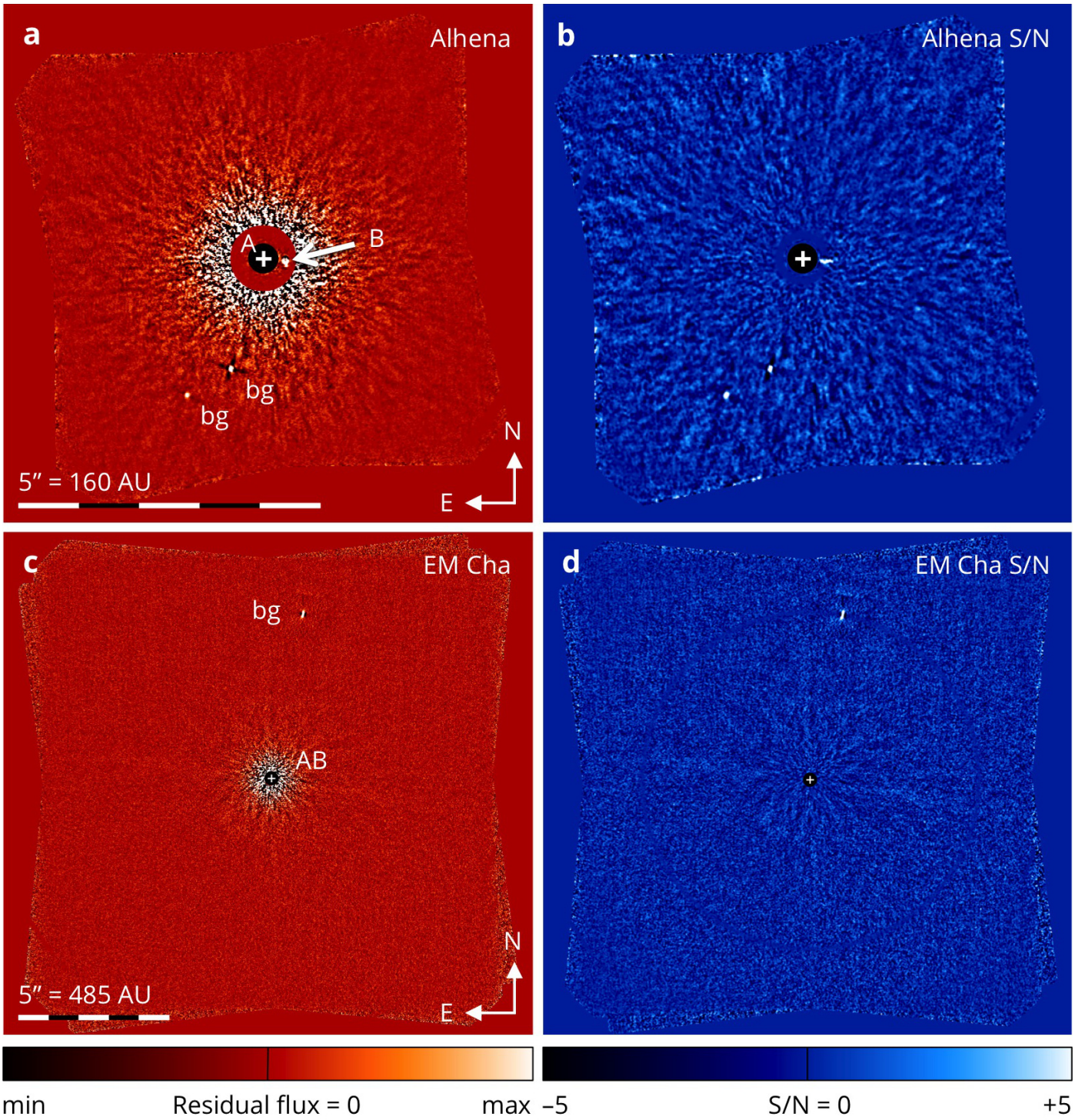

Fig. 1. Sample high-contrast H-band images from the SPOTS pilot survey taken on VLT NaCo. **(a)** LOCI ADI image of Alhena at linear stretch of $\pm 7 \times 10^{-7}$ times the primary star's peak flux. The image is centered on the A-type primary star (marked with a plus sign and the label A). The area within 0.″55 of the primary is displayed with a software attenuation of a factor of 1/1000 in order to render the resolved G-type secondary star (marked B) visible. Despite the presence of the secondary, the ADI processing effectively removes the primary's PSF, revealing two faint point sources nearby. Our follow-up observations identify these sources as background stars (marked bg). If they had been co-moving companions sharing the host system's age, their H-band brightness would have corresponded to masses of 29 $M_{\rm Jup}$ and 45 $M_{\rm Jup}$ in the COND evolutionary models by Baraffe et al. (2003). The field of view read out from the detector was reduced for this observation to allow for faster readout times. **(b)** The signal-to-noise (S/N) ratio map corresponding to image (a), produced by cutting the image into concentric annuli and dividing their pixel values by their standard deviation, displayed at a linear stretch of $[-5, 5]\,\sigma$. Since the secondary star is much fainter than the primary, it does not disturb the well-behaved residual speckle noise pattern. **(c)** LOCI ADI image of EM Cha at a linear stretch of $\pm 2.2 \times 10^{-5}$ times the unresolved binary's peak flux. The location of the unresolved target binary is marked by a plus sign and the label AB. A known background star is visible (marked bg). Its brightness corresponds to a 7 $M_{\rm Jup}$ planet at the system age. **(d)** The S/N map corresponding to image (c), demonstrating well-behaved residual noise.

Target	Epoch	Integr. time (s)	Bin. res.?	Candidates & bkgd. obj. (hypothetical masses)	Follow-up needed?	Follow-up obtained?
ESO Program 088.C-0291(A)						
δ Cap	2011-10-06	1320		—		
IK Peg	2011-10-10	1938		$2 \times 7\,M_{\rm Jup}$ planet at large separation $1 \times 7\,M_{\rm Jup}$ planet near IWA ($4.9\,\sigma$)	■	□
HIP 12545	2011-10-31	2040		—		
TYC 5907 1244 1	2011-11-05	1224		—		
HIP 16853	2011-11-09	1596		$1 \times$ star		
HIP 9892	2011-12-03	960		$1 \times$ background galaxy		
EM Cha	2011-12-15	1428		$1 \times$ confirmed background star		
TYC 8569 3597 1	2011-12-17	1200		crowded field	■	
AF Lep	2011-12-20	1596		—		
Alhena	2011-12-22	1320	■	$2 \times$ brown dwarf	■	■
HIP 25709	2011-12-22	2520		—		
26 Gem	2012-01-13	1638		$1 \times$ high-mass brown dwarf at IWA	■	■
HIP 76629	2012-07-20	1672		crowded field	■	
ESO program 090.C-0416(B)						
V1136 Tau	2012-11-21	1560	■	$1 \times$ star		
TYC 6386 0896 1	2012-11-26	1224		—		
XZ Pic	2013-01-03	960		—		
UX For	2013-01-05	2280	■	—		
TYC 8104 0991 1	2013-01-07	1200		—		
HIP 47760	2013-01-24	1224		—		
TYC 6604 0118 1	2013-01-26	1224		—		
GS Leo	2013-02-10	1560		$1 \times 12\,M_{\rm Jup}$ planet near IWA	■	■
TYC 9399 2452 1	2013-03-03	1224		$1 \times 10\,M_{\rm Jup}$ planet	■	
HS Lup	2013-04-30	1596		3×6–$11\,M_{\rm Jup}$ planet	■	
HIP 78416	2013-05-11	720		$1 \times$ foreground star 4×5–$11\,M_{\rm Jup}$ planet $3 \times$ background galaxy	■	
CS Gru	2013-06-26	720		—		
BS Ind	2013-06-28	1560		2×3–$9\,M_{\rm Jup}$ planet	■	

Table 2. Status of SPOTS exploratory observations. A black square in the column "Bin. res.?" indicates that the target binary has been resolved in our images. In the last two columns, a black square indicates that follow-up observations were deemed necessary, and were successfully executed, respectively. The empty square for the target IK Peg marks a follow-up observations that was executed, but turned out to be insufficiently sensitive to re-detect the candidate sources. The acronym IWA stands for inner working angle, which, in this particular context, refers to the minimum angular separation from the star at which there is sufficient field rotation to perform LOCI ADI processing. Note that detections near the IWA suffer from increased false alarm probability due to small-number statistics (Mawet et al. 2014). Background galaxies are identified by their visibly extended morphology that is inconsistent with the stellar PSF observed in the unsaturated calibration frames. None of the targets with reliable follow-up observations have yielded any co-moving companions.

and inner working angle (IWA)[1] than from Paranal. In the first-epoch data, the candidate appeared as a $6\,\sigma$ signal at a separation of $0\farcs4$ from the star, very close to the inner working angle given by the poor field rotation range of those data. Although the follow-up data provided twice the contrast performance of the first-epoch data at the location of the candidate and offered a significantly smaller inner working angle, the candidate signal was not re-detected. We conclude that the candidate was a deviant residual speckle from the ADI data reduction in the first epoch, rather than a real on-sky source. At the IWA, the number of frames available to the ADI algorithm for PSF subtraction is extremely limited, thus the residual noise can no longer be assumed to approximate Gaussian statistics as is commonly the case in the well-sampled parts of an ADI output image (Mawet et al. 2014). The apparent $6\,\sigma$ significance in the first-epoch image may therefore have been overestimated.

[1] While the term IWA originates from coronography, we use it to refer to the minimum angular separation from the star at which the total field rotation is sufficient to perform LOCI ADI for a given dataset.

4.3. Preliminary results from the planet search

Since many targets whose exploratory observations revealed promising companion candidates remain without a second epoch and therefore cannot yet be tested for common proper motion, we defer an in-depth report and statistical analysis of the results to a future paper. Since NaCo is scheduled to be offered again on VLT in ESO period P94, the remaining follow-up observations could be concluded by early 2015 at the earliest.

In the meantime, the current body of observations constitute a successful pilot run for the full SPOTS survey, demonstrating the feasibility and validity of our observational strategy. Most of our targets are unresolved spectroscopic binaries, which behave like single stars for the purpose of observation and data reduction. As the images of Alhena in Figure 1 demonstrate, even tar-

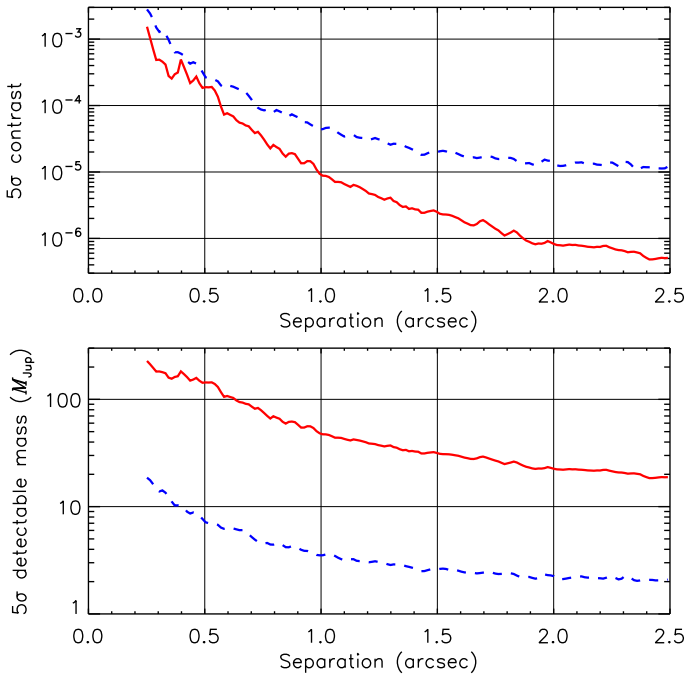

Fig. 2. Plot of the $5\,\sigma$ contrast (top panel) and the corresponding $5\,\sigma$ minimum detectable planet mass (bottom panel) for the LOCI ADI images from the two sample targets Alhena (red solid lines) and EM Cha (blue dashed lines). Both curves are corrected for the partial loss of planet flux due to self-subtraction in the data reduction. The total amount of field rotation captured was low in both observations (11.8° for Alhena and 12.6° for EM Cha); thus, the curves are conservative representations of the survey's sensitivity. Note that Alhena provides higher contrast than EM Cha since it is a brighter star and therefore offers more dynamic range between the stellar peak flux and the background sensitivity limit. On the other hand, since EM Cha is a much younger system than Alhena (8 Myr vs. 300 Myr), the minimum detectable companion masses are lower for EM Cha by an order of magnitude.

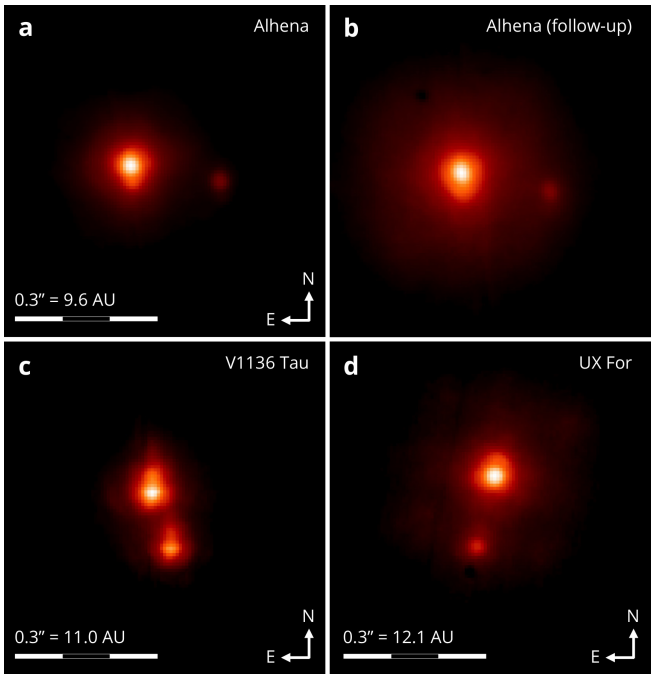

Fig. 3. Resolved multiple targets from the NaCo-based stage of the SPOTS survey: **(a)** Alhena (= γ Gem; exploratory observation), **(b)** Alhena (follow-up observation), **(c)** V1136 Tau, suffering some degraded AO correction, **(d)** UX For, showing the bright unresolved AB binary and the fainter C tertiary. All images are shown at a logarithmic stretch spanning 2.2 orders of magnitude.

Target	Epoch	Sep. (mas)	PA (°)
Alhena	2011-12-22	381.9 ± 1.2	259.46 ± 0.16
	2013-03-02	378.4 ± 2.7	257.44 ± 0.57
V1136 Tau	2012-11-22	247.8 ± 0.5	197.74 ± 0.40
UX For	2013-01-02	305.8 ± 0.9	165.32 ± 0.43

Table 3. Relative astrometry of the three resolved target binaries in the NaCo-based stage of the SPOTS survey.

gets with a resolved secondary star are useful to search for planets with ADI, in particular if the secondary is much fainter than the primary. Of our 26 exploratory targets, 10 have been found to require follow-up, which coincides well with the follow-up rate of 30% found for single stars in the NaCo large program (Chauvin et al. 2014).

Among the three targets with reliable follow-up observations (Alhena, 26 Gem, GS Leo), no co-moving companion has been found. A total of seven targets with at least one candidate for a planetary-mass companion remain to be confirmed (IK Peg, TYC 8569 3597 1, HIP 76629, TYC 9399 2452 1, HS Lup, HIP 78416, BS Ind).

The final astrometric analyses will be published in the full survey paper foreseen for 2015.

4.4. Astrometry of resolved binary targets

As an auxiliary science result, our survey data provide accurate stellar astrometry for three resolved target binary systems: Alhena (two epochs), V1136 Tau, and UX For. Unsaturated images from these four observations are shown in Figure 3, demonstrating the clear detections. Each of these targets is briefly discussed in a dedicated paragraph below. The numerical results are summarized in Table 3.

For all targets, unsaturated frames taken as part of our high-contrast observing runs for the purpose of photometric calibration were used to measure the relative astrometry of the target binary. The position of each stellar component was extracted using the `gcntrd` function in `IDL`. The error of this measurement was estimated to the FWHM of the secondary's PSF divided by its S/N ratio. A second error contribution is due to the uncertainty in True North orientation and plate scale. Since the SPOTS observations are performed in service mode and distributed over the course of years, it was impractical to include regular astrometric calibration observations. For the first-epoch observation of Alhena, we use the calibration values reported for a roughly contemporary epoch in the NaCo Large Program (Chauvin et al. 2014; Table 5). For all epochs after early 2012, we adopt the last reported values (from 2012-01-02), which carry a considerable uncertainty in True North orientation. We represent this uncertainty with an error bar of 0.°4, spanning the full range of True North orientations reported between 2009-11-23 and 2012-01-02. The final errors on the position angle and separation of the secondary star are obtained by combining the centroiding and calibration errors in quadrature.

Alhena (= γ Gem, WDS J06377+1624Aa,Ab, HD 47105, HIP 31681) comprises an A-type primary and a G-type secondary. While constraints from Doppler spectroscopy and astrometric tracking of the system's photocenter had been available for

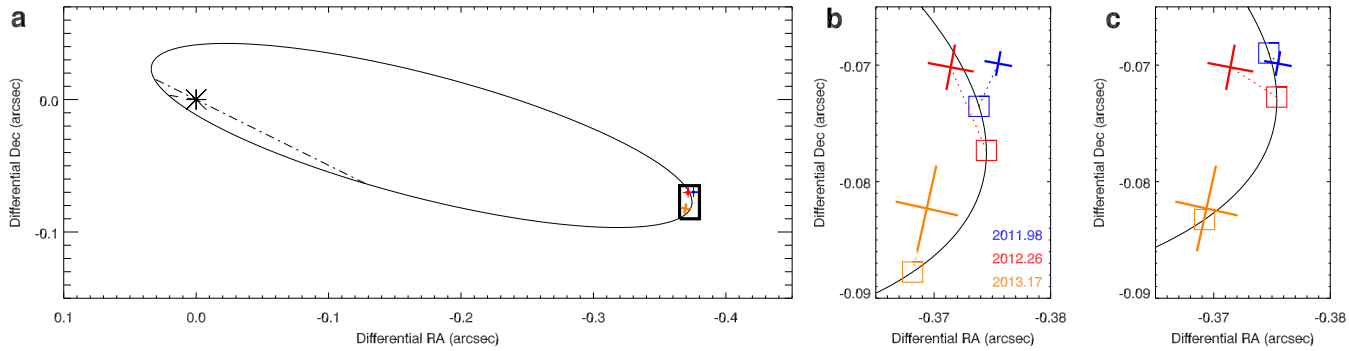

Fig. 4. Astrometry of the resolved binary target Alhena (= γ Gem). **(a)** Overview the orbit of Alhena B relative to Alhena A, as reported in Drummond (2014). The black rectangular frame indicates the area shown at larger magnification in the following panels. The position of Alhena A is marked with a star. **(b)** Observed relative positions of Alhena B (crosses) and their predicted positions (squares) on the assumed orbit for each of the three epochs (2011.98, 2013.17: this work; 2012.26: Drummond 2014). The sizes of the crosses correspond to the astrometric error bars in the azimuthal and radial directions. Note that the observed positions are systematically and significantly offset to the North ($\chi^2 = 31.4$). **(c)** The same for an adjusted orbit with $\Omega' = \Omega + 0\overset{\circ}{.}7$, leading to a good fit the data ($\chi^2 = 6.8$).

decades, the secondary star was only recently resolved for the first time (Drummond 2014), allowing these authors to propose a first complete orbital solution. Our exploratory and follow-up observations add two new epochs of relative astrometry, bracketing the single epoch of that author. In Figure 4, we illustrate the relative orbit of Alhena B around A as proposed in Drummond (2014), and the three resolved astrometric measurements. All data points appear to be systematically and significantly offset from their expected locations to the North ($\chi^2 = 31.4$). While refitting the orbit to all published constraints is beyond the scope of this work, we note that adding $+0\overset{\circ}{.}7$ to the longitude of the ascending node, Ω, removes these discrepancies and yields a good fit ($\chi^2 = 6.8$) without impacting the Doppler spectroscopy constraints (Figure 4c).

V1136 Tau (= CHR 14, HD 284163, WDS J04119+2338AB, HIP 19591) is listed with a period of $P = 40.9$ yr, a semi-major axis of $a = 0\overset{''}{.}31$, and an eccentricity of $e = 0.853$ in Malkov et al. (2012a). Both component stars appear elongated towards the North in our images, likely due to an imperfect PSF shape caused by wave-front sensing on the resolved, low-contrast binary guide star. Our astrometry places the secondary star between the positions reported for a bracketing pair of epochs by Tokovinin et al. (2012, 2014).

UX For (= HIP 12716, HD 17084, TOK 187) is a triple system comprising an unresolved G6V-type spectroscopic binary with a 0.955-day period and a resolved tertiary component first reported in Hartkopf et al. (2012a). No orbital solution is given, though the period of the tertiary is estimated to 40 years.

5. Conclusion

SPOTS (Search for Planets Orbiting Two Stars) is the first dedicated high-contrast imaging survey aimed at sampling the population of giant planets on wide circumbinary orbits. In this work (Paper I), we have presented our scientific rationale for this kind of survey, which can be summarized in four points:

- Theoretical and observational work predicts that giant planets can form, evolve, and survive on long time scales in circumbinary environments. However, most direct imaging surveys so far have excluded binaries from their target lists, leaving this interesting demographic of planets largely unexplored.
- Close binary systems that make promising hosts for circumbinary planets do not cause difficulties in direct imaging observations or data reduction. Furthermore, a binary host star may offer more planet-forming resources than a single star of the same overall brightness.
- Circumbinary planets may be scattered or continuously pushed out to larger orbital radii by dynamic interaction with their host binary, enriching the population of wide-orbit planets.
- Since binarity of the host star influences planet formation by core accretion and gravitational instability in different ways, sampling the circumbinary planet demography may yield new and unique insights into the processes of planet formation.

Furthermore, we have presented the design and current status of the SPOTS survey. In the context of our pilot survey on VLT NaCo, we have obtained exploratory observations of 26 targets, and are currently in the process of concluding the follow-up efforts for the promising companion candidates in that sample. Our preliminary results demonstrate the feasibility and validity of our observing strategy. No confirmed co-moving companion has been discovered so far; however, seven targets with promising candidates remain to be re-observed for common proper motion testing (cf. Section 4.3).

Finally, we have reported on the astrometry of the three resolved binaries in our observed sample (Alhena, V1136 Tau, UX For).

In a separate publication (Paper II), we present a statistical analysis of the direct imaging constraints on tight binary targets collected from the target lists of several published surveys.

A full report and statistical analysis for this NaCo-based stage of the SPOTS survey will be delivered in a third publication upon completion of the follow-up observations (expected in 2015). A second stage of the SPOTS survey comprising 40 more targets is then foreseen with VLT SPHERE in the following years.

Acknowledgements. The authors thank David Lafrenière for providing the source code for his LOCI algorithm, and the anonymous referee for useful comments. CTh is supported by the European Commission under the Marie Curie IEF grant No. 329875, and JCa by the U.S. National Science Foundation under award No. 1009203. SD and MB ackowledge support from PRIN-INAF "Planetary systems at young ages". The authors thank the ESO Paranal staff for their assistance and execution of service-mode observations. The authors wish to recognize and acknowledge the very significant cultural role and reverence that the

summit of Mauna Kea has always had within the indigenous Hawaiian community. We are most fortunate to have the opportunity to conduct observations from this mountain.

References

Allard, F., Hauschildt, P. H., Alexander, D. R., Tamanai, A., & Schweitzer, A. 2001, ApJ, 556, 357
Armstrong, D. J., Osborn, H., Brown, D., et al. 2014, ArXiv e-prints
Artymowicz, P. & Lubow, S. H. 1994, ApJ, 421, 651
Bailey, III, J. I., White, R. J., Blake, C. H., et al. 2012, ApJ, 749, 16
Baraffe, I., Chabrier, G., Barman, T. S., Allard, F., & Hauschildt, P. H. 2003, A&A, 402, 701
Bender, C. F. & Simon, M. 2008, ApJ, 689, 416
Bergfors, C., Brandner, W., Daemgen, S., et al. 2013, MNRAS, 428, 182
Beuermann, K., Hessman, F. V., Dreizler, S., et al. 2010, A&A, 521, L60
Biller, B. A., Liu, M. C., Wahhaj, Z., et al. 2010, ApJ, 720, L82
Biller, B. A., Liu, M. C., Wahhaj, Z., et al. 2013, ApJ, 777, 160
Bonavita, M., Chauvin, G., Desidera, S., et al. 2011, ArXiv e-prints
Bonavita, M. & Desidera, S. 2007, A&A, 468, 721
Bonavita, M., Desidera, S., Thalmann, C., et al. 2014, in prep. (Paper II)
Bonnefoy, M., Boccaletti, A., Lagrange, A.-M., et al. 2013, A&A, 555, A107
Boss, A. P. 2006, ApJ, 641, 1148
Carson, J., Thalmann, C., Janson, M., et al. 2013, ApJ, 763, L32
Chauvin, G., Beust, H., Lagrange, A.-M., & Eggenberger, A. 2011, A&A, 528, A8
Chauvin, G., Vigan, A., Bonnefoy, M., et al. 2014, ArXiv e-prints
Christian, D. J., Mathioudakis, M., & Vennes, S. 2002, Information Bulletin on Variable Stars, 5281, 1
Covino, E., Alcala, J. M., Allain, S., et al. 1997, A&A, 328, 187
Crepp, J., Serabyn, E., Carson, J., Ge, J., & Kravchenko, I. 2010, ApJ, 715, 1533
Cutispoto, G., Pastori, L., Pasquini, L., et al. 2002, A&A, 384, 491
Cutispoto, G., Pastori, L., Tagliaferri, G., Messina, S., & Pallavicini, R. 1999, A&AS, 138, 87
Dall, T. H., Foellmi, C., Pritchard, J., et al. 2007, A&A, 470, 1201
Davis, P. J., Kolb, U., & Willems, B. 2010, MNRAS, 403, 179
Delorme, P., Gagné, J., Girard, J. H., et al. 2013, A&A, 553, L5
Desidera, S. & Barbieri, M. 2007, A&A, 462, 345
Desidera, S., Covino, E., Messina, S., et al. 2014, ArXiv e-prints
Desidera, S., Gratton, R. G., Lucatello, S., Claudi, R. U., & Dall, T. H. 2006, A&A, 454, 553
Doyle, L. R., Carter, J. A., Fabrycky, D. C., et al. 2011, Science, 333, 1602
Drummond, J. D. 2014, AJ, 147, 65
Duchêne, G., Bouvier, J., Bontemps, S., André, P., & Motte, F. 2004, A&A, 427, 651
Dutrey, A., Guilloteau, S., & Simon, M. 1994, A&A, 286, 149
Eggenberger, A., Udry, S., Chauvin, G., et al. 2007, A&A, 474, 273
Evans, D. S. 1961, Royal Greenwich Observatory Bulletins, 30, 93
Gagné, J., Lafrenière, D., Doyon, R., Malo, L., & Artigau, É. 2014, ApJ, 783, 121
Galland, F., Lagrange, A.-M., Udry, S., et al. 2005, A&A, 443, 337
Griffin, R. F. & Gunn, J. E. 1981, AJ, 86, 588
Guenther, E. W., Covino, E., Alcalá, J. M., Esposito, M., & Mundt, R. 2005, A&A, 433, 629
Guenther, E. W. & Esposito, E. 2007, ArXiv Astrophysics e-prints
Haghighipour, N., ed. 2010, Astrophysics and Space Science Library, Vol. 366, Planets in Binary Star Systems
Hartkopf, W. I., Tokovinin, A., & Mason, B. D. 2012a, AJ, 143, 42
Hartkopf, W. I., Tokovinin, A., & Mason, B. D. 2012b, AJ, 143, 42
Hatzes, A. P., Cochran, W. D., Endl, M., et al. 2003, ApJ, 599, 1383
Helt, B. E. & Jensen, K. S. 1989, Information Bulletin on Variable Stars, 3306, 1
Holman, M. J. & Wiegert, P. A. 1999, AJ, 117, 621
Horner, J., Wittenmyer, R. A., Hinse, T. C., et al. 2013, MNRAS, 435, 2033
Janson, M., Brandt, T. D., Moro-Martín, A., et al. 2013, ApJ, 773, 73
Jones, H. R. A., Paul Butler, R., Marcy, G. W., et al. 2002, MNRAS, 337, 1170
Kennedy, G. M. & Kenyon, S. J. 2008, ApJ, 673, 502
Kley, W. & Haghighipour, N. 2014, A&A, 564, A72
Kobayashi, N., Tokunaga, A. T., Terada, H., et al. 2000, in Society of Photo-Optical Instrumentation Engineers (SPIE) Conference Series, Vol. 4008, Optical and IR Telescope Instrumentation and Detectors, ed. M. Iye & A. F. Moorwood, 1056–1066
Konacki, M., Muterspaugh, M. W., Kulkarni, S. R., & Hełminiak, K. G. 2009, ApJ, 704, 513
Kuzuhara, M., Tamura, M., Kudo, T., et al. 2013, ApJ, 774, 11
Lafrenière, D., Doyon, R., Marois, C., et al. 2007a, ApJ, 670, 1367
Lafrenière, D., Marois, C., Doyon, R., Nadeau, D., & Artigau, É. 2007b, ApJ, 660, 770
Lagrange, A.-M., Bonnefoy, M., Chauvin, G., et al. 2010, Science, 329, 57
Lee, J. W., Kim, S.-L., Kim, C.-H., et al. 2009, ApJ, 137, 3181
Lyo, A.-R., Lawson, W. A., Mamajek, E. E., et al. 2003, MNRAS, 338, 616
Makarov, V. V. 2007, ApJ, 654, L81
Makarov, V. V. & Kaplan, G. H. 2005, ApJ, 129, 2420
Malkov, O. Y., Tamazian, V. S., Docobo, J. A., & Chulkov, D. A. 2012a, A&A, 546, A69
Malkov, O. Y., Tamazian, V. S., Docobo, J. A., & Chulkov, D. A. 2012b, A&A, 546, A69
Malo, L., Doyon, R., Lafrenière, D., et al. 2013, ApJ, 762, 88
Marcy, G., Butler, R. P., Fischer, D., et al. 2005, Progress of Theoretical Physics Supplement, 158, 24
Marois, C., Lafrenière, D., Doyon, R., Macintosh, B., & Nadeau, D. 2006, ApJ, 641, 556
Marois, C., Zuckerman, B., Konopacky, Q. M., Macintosh, B., & Barman, T. 2010, Nature, 468, 1080
Marsh, T. R., Parsons, S. G., Bours, M. C. P., et al. 2014, MNRAS, 437, 475
Martin, R. G., Armitage, P. J., & Alexander, R. D. 2013, ApJ, 773, 74
Martin, R. G., Lubow, S. H., Pringle, J. E., & Wyatt, M. C. 2007, MNRAS, 378, 1589
Marzari, F., Thebault, P., Scholl, H., Picogna, G., & Baruteau, C. 2013, A&A, 553, A71
Mathieu, R. D. 1992, in IAU Symposium, Vol. 151, Evolutionary Processes in Interacting Binary Stars, ed. Y. Kondo, R. Sistero, & R. S. Polidan, 21
Mawet, D., Milli, J., Wahhaj, Z., et al. 2014, ArXiv e-prints
Mayer, L., Wadsley, J., Quinn, T., & Stadel, J. 2005, MNRAS, 363, 641
Meschiari, S. 2012, ApJ, 761, L7
Nelson, R. P. 2003, MNRAS, 345, 233
Neuhauser, R. & Brandner, W. 1998, A&A, 330, L29
Neuhäuser, R., Guenther, E. W., Alves, J., et al. 2003, Astronomische Nachrichten, 324, 535
Nielsen, E. L. & Close, L. M. 2010, ApJ, 717, 878
Nielsen, E. L., Liu, M. C., Wahhaj, Z., et al. 2013, ApJ, 776, 4
Nordström, B., Mayor, M., Andersen, J., et al. 2004, A&A, 418, 989
Orosz, J. A., Welsh, W. F., Carter, J. A., et al. 2012, Science, 337, 1511
Pallavicini, R., Randich, S., & Giampapa, M. S. 1992, A&A, 253, 185
Pascucci, I., Apai, D., Hardegree-Ullman, E. E., et al. 2008, ApJ, 673, 477
Perets, H. B. 2010, ArXiv e-prints
Pierens, A. & Nelson, R. P. 2008, A&A, 483, 633
Pierens, A. & Nelson, R. P. 2013, A&A, 556, A134
Rafikov, R. R. 2013, ApJ, 764, L16
Raghavan, D., McAlister, H. A., Henry, T. J., et al. 2010, ApJS, 190, 1
Rameau, J., Chauvin, G., Lagrange, A.-M., et al. 2013a, A&A, 553, A60
Rameau, J., Chauvin, G., Lagrange, A.-M., et al. 2013b, ArXiv e-prints
Song, I., Zuckerman, B., & Bessell, M. S. 2003, ApJ, 599, 342
Surkova, L. P. & Svechnikov, M. A. 2004, VizieR Online Data Catalog, 5115, 0
Tamura, M. 2009, in American Institute of Physics Conference Series, Vol. 1158, American Institute of Physics Conference Series, ed. T. Usuda, M. Tamura, & M. Ishii, 11–16
Thalmann, C., Carson, J., Janson, M., et al. 2009, ApJ, 707, L123
Thalmann, C., Desidera, S., Bergfors, C., et al. 2013, in Protostars and Planets VI, Heidelberg, July 15-20, 2013. Poster #2K012, 12
Thebault, P. 2011, Celestial Mechanics and Dynamical Astronomy, 111, 29
Tokovinin, A., Hartung, M., Hayward, T. L., & Makarov, V. V. 2012, AJ, 144, 7
Tokovinin, A., Mason, B. D., & Hartkopf, W. I. 2014, AJ, 147, 123
Torres, C. A. O., Quast, G. R., da Silva, L., et al. 2006, A&A, 460, 695
Torres, C. A. O., Quast, G. R., Melo, C. H. F., & Sterzik, M. F. 2008, Young Nearby Loose Associations, ed. Reipurth, B., 757
Torres, G., Guenther, E. W., Marschall, L. A., et al. 2003, ApJ, 125, 825
Trilling, D. E., Stansberry, J. A., Stapelfeldt, K. R., et al. 2007, ApJ, 658, 1289
Veras, D. & Armitage, P. J. 2004, MNRAS, 347, 613
Vigan, A., Patience, J., Marois, C., et al. 2012, A&A, 544, A9
Wang, J., Xie, J.-W., Barclay, T., & Fischer, D. A. 2014, ApJ, 783, 4
Washuettl, A. & Strassmeier, K. G. 2001, A&A, 370, 218
Welsh, W. F., Orosz, J. A., Carter, J. A., & Fabrycky, D. C. 2013, ArXiv e-prints
Wonnacott, D., Kellett, B. J., & Stickland, D. J. 1993, MNRAS, 262, 277
Wright, J. T., Fakhouri, O., Marcy, G. W., et al. 2011, PASP, 123, 412
Wright, J. T., Marcy, G. W., Butler, R. P., & Vogt, S. S. 2004, ApJS, 152, 261
Zuckerman, B., Rhee, J. H., Song, I., & Bessell, M. S. 2011, ApJ, 732, 61
Zuckerman, B. & Song, I. 2004, ARA&A, 42, 685

Appendix A: Discussion of individual targets

HIP 9892 = HD 13183: Member of Tucana association, classified as a long-period SB by Guenther & Esposito (2007). No orbital solution is available.

HIP 12545 = BD +05 0378: Member of β Pic moving group. Identifed as SB1 in Song et al. (2003) (peak-to-valley variation of 20 km/s, no orbital solution provided). However, Bailey et al. (2012) found no evidence for large RV variations from their monitoring over 600 days (14 epochs, scatter of 179 m/s). These observations might be explained by a high-eccentricity orbit.

UX For = HIP 12716 = HD 17084: Triple system formed by a close SB2 (orbital period 0.9548 d, mass ratio 1.371; Washuettl & Strassmeier 2001) and an outer component, resolved by Hartkopf et al. (2012b) and our own NACO observations, which is likely responsible of the proper motion difference between Hipparcos and historical proper motions (Makarov & Kaplan 2005). The large activity levels are likely due to tidal locking of the inner components, as the Lithium equivalent width (Li EW) is similar to that of the Hyades. The presence of the third component significantly limits the parameter space of possible planets around the central pair.

HIP 16853 = HD 22705: Member of Tucana association. Astrometric orbit and parallax adopted from Makarov (2007).

V1136 Tau = CHR 14 = HD 284163 = HIP 19591: Triple system, member of the Hyades. A 2.39 d RV orbit has been derived by Griffin & Gunn (1981), with indication of the presence of a tertiary companion from the presence in the spectra of an additional system of lines at constant radial velocity. The inner pair was resolved as SB2 thanks to NIR RVs by Bender & Simon (2008), yielding a mass ratio of 0.68 ± 0.03. The third component was visually resolved allowing a preliminary estimate of the orbit (Malkov et al. 2012b). The tertiary component is also identified in our NACO images (see Section 4).

TYC 5907-1244-1 = BD-20 951: Member of Tucana associaton and SB2 following Torres et al. (2008). No orbital solution is available.

AF Lep = HIP 25486 = HD 35850: Member of β Pic moving group. Reported as SB2 in Nordström et al. (2004), with mass ratio between the components of 0.72. Details of orbital solution not provided.

HIP 25709 = HD 36329: Member of Columba association, was reported as a SB2 with similar components by Torres et al. (2008). The orbital solution is not available.

XZ Pic = HIP 27134 = CD-59 1125: Short-period SB1 according to sparse RV measurements (Dall et al. 2007; Torres et al. 2006; Cutispoto et al. 1999). Age indicators based on activity and rotation are likely biased by tidal locking between the components. The lithium in the spectrum indicates an age of about 300 Myr.

26 Gem = HIP 32104 = HD 48097 = HR 2466: Member of Columba association according to Zuckerman et al. (2011) and Malo et al. (2013). Spectroscopic (Galland et al. 2005) and astrometric (Hipparcos orbital solution) binary. Combining the spectroscopic solution with the inclination from Hipparcos results in a companion mass of $0.51 M_{\odot}$ at 1.87 AU. The secondary is most likely responsbile for the X-ray emission from the system.

Alhena = γ Gem = HIP 31681 = HD 47105: Spectroscopic, astrometric and close visual binary. The constraints on orbital solution derived from our own observations are presented in Section 4.4. The isochrone fitting yields an age of 300 Myr and the X-ray emission (assuming it comes from the late-type secondary) is consistent with such an estimate. The space velocities are close to those of the Ursa Major association.

TYC 8104-0991-1 = CD-45 2654: SB3 discovered by Torres et al. (2006), but no additional information is available on the binary parameters. The large Li EW indidates an age of about 100 Myr.

EM Cha = RECX7: SB2, member of η Cha open cluster. Masses and orbital parameters from Lyo et al. (2003) (eccentricity not provided, we assume 0.0 due the short period). The orbital period is equal to the photometric period, suggesting the occurrence of tidal locking.

TYC 8569-3597-1 = CD-53 2515: Member of Carina MG and SB2 with a period of 24.06 days (Torres et al. 2008). Distance from Torres et al. (2008).

GS Leo = HIP 46637 = HD 82159: Triple system, formed by a close pair and an outer component. The latter was observed by Chauvin et al. (2014). Stellar and binary parameters from Desidera et al. (2014).

TYC 9399-2452-1 = HD 81485B: The SB2 HD 81485B (Covino et al. 1997) is part of a quadruple system with HD 81485A and its close visual companion at $9'' \sim 500$ AU projected separation at the trigonometric distance of HD 81485A. The SB2 component shows exceptional high levels of chromospheric activity, while the primary is only moderately active (Desidera et al. 2006). This, together with the Li EW comparable with that of the Hyades (Torres et al. 2006), indicates an age of about 800 Myr and probable tidal-locking of the SB2 component. The very young age for the primary (14 Myr) derived from isochrone fitting by Neuhauser & Brandner (1998) is probably due to the unrecognized (at that time) multiplicity of A, that is actually overluminous by about 0.5 mag in K-band with respect to the individual Aa component. Finally, we note discrepant trigonometric parallaxes between the two reductions of Hipparcos data.

HIP 47760 = HD 84323: Star flagged as SB1 in Cutispoto et al. (2002) without further details. No orbital solution is available. The Li EW larger than Pleiades of similar colors and similar to that of member of Tucana association but the lack of system RV prevents a proper evaluation of MG membership. The BANYAN II online tool (Gagné et al. 2014) without using RV information does not support membership in any of the MG considered in that work. We adopt an age of 30 Myr.

TYC 6604-0118-1 = CD-22 7788 = BD-21 2961: Short-period (1.83 d) SB2 (Torres et al. 2003). The Li EW indicate an age pf about 100 Myr and the kinematic parameters are compatible with such a moderately young age. The close pair has a wide common proper motion companion (2MASS J09590930-2239582) at $26''$ projected separation.

HS Lup = HIP 74049 = HD 133822: SB2 with period 17.83 d (Evans 1961). There is independent evidence that the star is rather young, as it is active with a possible rotation period which is different from the orbital one (Helt & Jensen 1989) and shows lithium intermediate between that of members of Hyades and Pleiadesof similar color. We adopt an age of 250 Myr.

HIP 76629 = HD 139084 = V343 Nor: Triple system, member of β Pic MG. Evidence of RV variability is derived in the literature from Guenther & Esposito (2007) and Torres et al. (2006).

Including RVs measured on archival FEROS and HARPS spectra, we derived a tentative orbital solution with a period of about 4.5 years and moderate eccentricity (0.5–0.6). The corresponding minimum mass of the companion is 0.11 $M_{\odot}$. There is an additional companion, the M5Ve star HD 139084B at 10″.

HIP 78416 = HD 143215: Triple system, formed by an SB2 system discovered by Desidera et al. (2006) and a wide companion at 6.″55 (550 AU projected separation). The system is formed by three stars with similar masses. The large X-ray emission might be due to fast rotation due to tidal circularization. However, the isolated secondary also shows a fast rotational velocity, Ca II HK emission level similar to Pleiades, and a Lithium 6708 Å line stronger than Pleiades stars of similar color. Li lines are clearly visible and well separated also in the SB2 component. The star is at a distance of 84 ± 12 pc in front of the Lupus cloud. The kinematical parameters and the space position are compatible with those of Upper Centaurus Lupus (UCL) group. The age resulting from lithium is also fully compatible with UCL membership.

BS Ind = HIP 105404 = HD 202917: This is a spectroscopic binary with P = 3.3 yr and e = 0.6, in which the primary is found to be itself an eclipsing binary with P = 0.43 days. The components of the eclipsing system are likely late K- or early M-type stars, with a total mass of about 0.9 $M_{\odot}$, while the wider spectroscopic companion is a K0V-type star of 0.8$M_{\odot}$ (see Guenther et al. 2005, for all the details). Membership to Tuc-Hor association was supported by Zuckerman & Song (2004) and Malo et al. (2013) but rejected by Torres et al. (2008). The Li EW suggests an age as young as 10 Myr but should be taken with caution because of the composite nature of the system. We adopt Tuc-Hor membership and its age.

IK Peg = HIP 105860 = HD 204188: Single-lined SB with a massive white dwarf companion (Wonnacott et al. 1993). The system should have evolved through the common envelope phase, rendering it challenging to estimate the original configuration and the age of the system (Davis et al. 2010). The position of the primary close to the zero-age main sequence, the large mass and hot temperature of the white dwarf, and the young-disk kinematics support a moderately young age. Trilling et al. (2007) adopt an age of 100 Myr. The primary is also a δ Scu pulsating variable.

δ Cap = HIP 107556 = HD 207098 = GJ 837: Short-period spectroscopic and semi-detached eclipsing binary. Orbit from SB9: P = 1.02 d, e = 0.01, $K1$ = 70.80 km/s. In the catalog of semi-detached binaries (Surkova & Svechnikov 2004) individual masses and radii M_A = 1.50, M_B = 0.56, R_A = 1.85, R_B = 1.56 are listed. The large X-ray luminosity of the system is likely due to tidal-spin up of the late type secondary. An age of 540 Myr is derived by Nielsen et al. (2013). However, it is highly uncertain. Furthermore, the position on CMD and then age from iscochrone may have been altered by mass trasfer process. The kinematic parameters are compatible with a young age.

CS Gru = HIP 109901 = HD 211087: Lithium-rich K-type dwarf identified as SB1 (RMS of RV 37 km/s, 4 measurements) in SACY. The possibility of a tidally-locked binary can not be excluded from current data, but the large lithium EW indicates an age of about 100 Myr. The large uncertainty in the kinematic parameters due to the RV variability prevents a proper evaluation of membership to associations.

TYC 6386-0896-1 = HD 215341: SB2 discovered by Christian et al. (2002); the orbital solution is not available. The very large coronal and chromospheric activity are likely due to tidal locking, while Lithium is within the locus of Pleides stars. We adopt an age of 150 Myr.